SPARSE AND LOW-RANK DECOMPOSITION OF MR ARTIFACT IMAGES USING ANNIHILATING FILTER-BASED HANKEL MATRIX

Kyong Hwan Jin, Juyoung Lee, Dongwook Lee, Jong Chul Ye

Bio-Imaging and Signal Processing Lab., Dept. Bio & Brain Engineering
Korea Advanced Institute of Science & Technology (KAIST)
Email : jong.ye@kaist.ac.kr

ABSTRACT

In this paper, we propose a sparse and low-rank decomposition of annihilating filter-based Hankel matrix for MRI artifact removal. Based on the observation that some MR artifacts are originated from k-space outliers, we employ the recently proposed image modeling method using annihilating filter-based low-rank Hankel matrix approach (ALOHA) to decompose the sparse outliers from the low-rank component. Unlike the recent sparse and low rank decomposition for dynamic MRI, the proposed approach can be applied even for static images, because the k-space low rank component comes from the intrinsic image properties. We demonstrate that the proposed algorithm clearly removes several types of artifacts such as impulse noises, motion artifacts, and herringbone artifacts from MR images.

Index Terms— MRI artifacts, Hankel matrix, annihilation filter, sparse and low-rank decomposition, robust principal component anlaysis

1. INTRODUCTION

Many types of MR image artifacts are originated from outliers in k-space measurements. For example, herringbone artifacts (also called as crisscross artifact or corduroy artifact) are scattered all over the image in a single slice or multiple slices, which makes the images unusable. The main origin of this artifact is from electromagnetic spikes by gradient coils or fluctuating power supply which usually results in outliers in k-space measurement domain. Motion artifacts are also commonly observed when a subject moves during the scanning. Due to the movement during k-space scanning, some of the k-space data lose their integrity from the previous k-space data, which can be also considered as outliers.

In this paper, we propose a sparse and low rank decomposition algorithm for removal of MRI artifacts. By utilizing the recently proposed annihilating filter-based low rank Hankel matrix (ALOHA) approach for image modeling [1, 2], this paper shows that many MR artifacts can be decomposed into sparse outliers whereas k-space data from the underlying artifact-free image can be decomposed as a low-rank component of the Hankel matrix.

We are aware that sparse and low rank decomposition was recently proposed for the reconstruction of accelerated dynamic MR imaging [3]. In this approach, the static background was decomposed as a low rank component, whereas dynamic changes were decomposed into sparse components. However, the main difference of the proposed method from the previous work [3] is that our model works even for a static image without exploiting the temporal redundancies, because the low rankness in Hankel matrix is an inherent image property [1, 2]. Moreover, unlike the decomposition of static and dynamic images in [3], the sparse component in our method turns out to be artifact related signals and the low-rank component corresponds to the artifact-free image, so we can effectively remove the image artifacts and recover the accurate image reconstruction. The algorithm can be applied for both accelerated compressed sensing MRI and fully sampled MR acquisition. The experimental results using both retrospective and in vivo measurements demonstrate excellent performance in removing MRI artifacts.

2. THEORY

2.1. MR k-space Artifacts

MR raw data measurements are acquired by sampling echo signals corresponding to the k-space trajectories. Therefore, hardware imperfectness during the signal acquisition may corrupt k-space data. For example, artifacts such as RF overflow, DC offset, k-space spikes and RF interferences all corresponds to this type of k-space artifacts. Usually, these artifacts are encountered infrequently rather than in a continuous manner, so the resulting k-space artifacts are usually observed as sparse outliers.

Therefore, if there exists an algorithm to decompose the sparse outliers from the k-space samples, there is a chance to remove the artifacts. However, one of the technical hurdles in extracting k-space outlier is that it is difficult to differen-

This work is supported by the grant from Korean Goverment (NRF-2014R1A2A1A11052491).

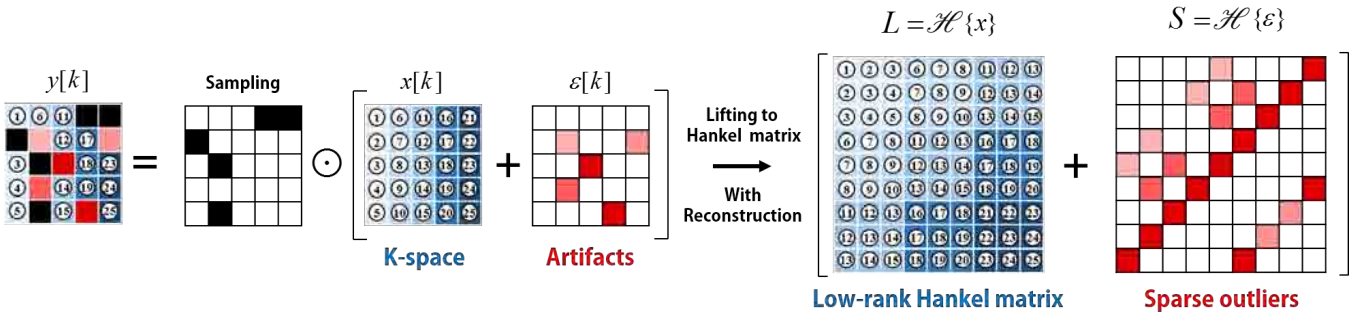

Fig. 1. Lifting of MR k-space data with artifacts to a Hankel structured matrix composed of low rank and sparse components.

tiate from the artifact-free k-space data. One of the most remarkable findings is, however, that if we form an annihilating filter-based Hankel matrix using the k-space data as shown in [1], then the artifact-free data and k-space outliers can be easily decomposed. In this section, we provide a description of the proposed sparse + low-rank decomposition of annihilating filter-based Hankel matrix that serves the goals. First, we start with the review of ALOHA [1, 2].

2.2. ALOHA : A Review

Recently, annihilating filter based low rank Hankel matrix approach (ALOHA) was proposed as a powerful tool for compressed sensing MRI [1] and image processing [2]. More specifically, if the signal $x(\mathbf{r})$ is sparse, then there exist an annihilating function $h(\mathbf{r})$ such that

$$x(\mathbf{r})h(\mathbf{r}) = 0 \overset{FT}{\longleftrightarrow} \widehat{x}(\mathbf{k}) * \widehat{h}(\mathbf{k}) = 0., \tag{1}$$

where $\widehat{x}(\mathbf{k})$ denotes the Fourier transform of $x(\mathbf{r})$. In particular, if $x(\mathbf{r})$ is represented as sum of Diracs, then $\widehat{h}(\mathbf{k})$ becomes a finite impulse response filter [1, 4]. Thus, Eq. (1) can be rewritten as matrix-vector form :

$$\mathscr{H}\{\widehat{x}\}\mathbf{h} = 0, \tag{2}$$

where $\mathscr{H}\{\cdot\}$ is Hankel matrix and $\mathbf{h}$ is the reverse ordered, vectorized annihilating filter. From this equation, we observe that Hankel matrix $\mathscr{H}\{\widehat{x}\}$ has null space and is low-ranked. This model can be generalized to signals that can be sparsified in a transform domain. Specifically, if the image can be sparsified using wavelets, then the low-rank Hankel matrix can be constructed for each band using weighted k-space data with wavelet weighting [1].

2.3. Robust ALOHA for MR Artifacts

As previously mentioned, some artifacts in MRI can be modeled as k-space sparse outliers. Accordingly, MRI measurements $\widehat{y}(\mathbf{k})$ can be modeled as

$$\widehat{y}(\mathbf{k}) = \widehat{x}(\mathbf{k}) + \widehat{\epsilon}(\mathbf{k}), \tag{3}$$

where $\widehat{x}(\mathbf{k})$ is a k-space data of artifact-free image and $\widehat{\epsilon}(\mathbf{k})$ is sparse k-space outlier. In Eq. (3), if the underlying image is sparse, the first term has an annihilation property as reviewed in Eq. (1)-(2), whereas the second term is irrelevant with annihilation property because of irregular structures. This implies that we can use the annihilation property as a differentiation tool between MRI artifacts and true MR images.

In general, an image is not sparse by itself, but can be sparsified with a transform such as spatial domain wavelet transform. Then, the corresponding k-space data becomes

$$\widehat{y}(\mathbf{k}) \cdot \widehat{\psi}(\mathbf{k}) = \widehat{x}(\mathbf{k}) \cdot \widehat{\psi}(\mathbf{k}) + \widehat{e}(\mathbf{k}) \cdot \widehat{\psi}(\mathbf{k})$$

where $\widehat{\psi}(\mathbf{k})$ is the spectrum of a wavelet. Then, we can find an annihilating filter that annihilates $\hat{x}(\mathbf{k}) \cdot \hat{\psi}(\mathbf{k})$. Moreover, the wavelet spectrum-weighted sparse outlier is still sparse, so the second term remains sparse as in Eq. (3). Therefore, we exploit annihilation property to remove the sparse outliers. Specifically, this can be achieved by searching low-rank matrix from Hankel structured matrix. More specifically, we perform a lifting to a Hankel structured matrix. Then, we have

$$\mathscr{H}\{\widehat{\mathbf{Y}} \odot \widehat{\mathbf{W}}\} = \underbrace{\mathscr{H}\{\widehat{\mathbf{X}} \odot \widehat{\mathbf{W}}\}}_{\text{low-rank}} + \underbrace{\mathscr{H}\{\widehat{\mathbf{E}} \odot \widehat{\mathbf{W}}\}}_{\text{sparse outlier}}, \tag{4}$$

where $\mathscr{H}\{\cdot\}$ is Hankel matrix, $\odot$ is Hadamard product, and $\widehat{\mathbf{X}}$ and $\widehat{\mathbf{W}}$ denote the matrices constructed from discretized samples of $\widehat{x}(\mathbf{k})$ and $\widehat{\psi}(\mathbf{k})$, respectively. Here, note that the lifted Hankel matrix from sparse components is still sparse as shown in Fig. 1. Therefore, Eq. (4) becomes a structure for sparse + low-rank decomposition. Because RPCA (robust principal component analysis) [5] has been extensively investigated for decomposition of mixed matrix into low-rank and sparse components, we employ the main idea of RPCA method to decompose ALOHA matrix for a removal of MRI artifact. After sparse + low-rank decomposition, the weighted k-space for low-rank component is returned to original k-space by unweighting.

2.4. Optimization framework

The proposed sparse + low-rank decomposition of Hankel matrix was implemented using SVD-free ADMM method [1] as successfully demonstrated for impulse noise removal in images [6]. The minimization problem is then given by

$$\begin{aligned} \min_{\mathbf{M}} \quad & \|\mathscr{H}\{\mathbf{M}\}\|_* + \tau\|\mathbf{E}\|_1 \\ \text{subject to} \quad & \widehat{\mathbf{Y}} \odot \widehat{\mathbf{W}} = \mathbf{M} + \mathbf{E}, \end{aligned}$$

where $\mathbf{M}$ denote the weighted k-space samples without artifacts, $\mathbf{E}$ denote sparse outliers corresponding to MR artifacts, and τ denotes the trade-off parameter between the low rank components and outliers. The minimization problem can be reformulated by a non-constrained factorized nuclear norm minimization such as

$$\begin{aligned} L(\mathbf{U},\mathbf{V},\mathbf{E},\mathbf{M},\boldsymbol{\eta},\boldsymbol{\Gamma}) &= \frac{1}{2}\left(\|\mathbf{U}\|_F^2 + \|\mathbf{V}\|_F^2\right) + \tau\|\mathbf{E}\|_1 \\ &+ \frac{\beta}{2}\|\mathbf{M}+\mathbf{E}-\widehat{\mathbf{Y}}_w+\boldsymbol{\eta}\|_F^2 + \frac{\mu}{2}\|\mathscr{H}\{\mathbf{M}\}-\mathbf{U}\mathbf{V}^H+\boldsymbol{\Gamma}\|_F^2 \end{aligned}$$

where $\widehat{\mathbf{Y}}_w = \widehat{\mathbf{Y}} \odot \widehat{\mathbf{W}}$ and $\boldsymbol{\eta}$ and $\boldsymbol{\Gamma}$ are Lagrangian variables. Then, each subproblem is simply solved sequentially by following closed form solutions:

$$\begin{aligned} \mathbf{E}^{(k+1)} &= \mathcal{S}_{\tau/\beta}\left(\widehat{\mathbf{Y}}_w - \mathbf{M}^{(k)} - \boldsymbol{\eta}^{(k)}\right), \\ \mathbf{M}^{(k+1)} &= \frac{1}{\mu+\beta}\left(\mu\mathscr{H}^\dagger\left\{\mathbf{U}^{(k)}\mathbf{V}^{(k)H} - \boldsymbol{\Gamma}^{(k)}\right\}\right. \\ &\quad \left. -\beta\left(\mathbf{E}^{(k+1)} - \mathbf{Y}_w + \boldsymbol{\eta}^{(k)}\right)\right), \\ \mathbf{U}^{(k+1)} &= \mu\left(\mathscr{H}\{\mathbf{M}^{(k+1)}\} + \boldsymbol{\Gamma}^{(k)}\right)\mathbf{V}^{(k)}\left(I + \mu\mathbf{V}^{(k)H}\mathbf{V}^{(k)}\right)^{-1}, \\ \mathbf{V}^{(k+1)} &= \mu\left(\mathscr{H}\{\mathbf{M}^{(k+1)}\} + \boldsymbol{\Gamma}^{(k)}\right)^H\mathbf{U}^{(k+1)} \\ &\quad \cdot\left(I + \mu\mathbf{U}^{(k+1)H}\mathbf{U}^{(k+1)}\right)^{-1}, \\ \boldsymbol{\eta}^{(k+1)} &= \mathbf{M}^{(k+1)} + \mathbf{E}^{(k+1)} - \widehat{\mathbf{Y}}_w + \boldsymbol{\eta}^{(k)}, \\ \boldsymbol{\Gamma}^{(k+1)} &= \mathscr{H}\{\mathbf{M}^{(k+1)}\} - \mathbf{U}^{(k+1)}\mathbf{V}^{(k+1)H} + \boldsymbol{\Gamma}^{(k)}, \end{aligned}$$

where μ and β are trade-off parameters, $\mathcal{S}_\tau$ denotes the pixel-wise soft-thresholding with the value τ, $\mathscr{H}^\dagger$ corresponds to the mapping from Hankel structure to a original structure ($\mathscr{H}^\dagger = (\mathscr{H}^*\mathscr{H})^{-1}\mathscr{H}^*$).

3. RESULTS

To assess the performance of robust ALOHA for MRI artifact removal, we considered three types of artifacts, which include impulse noises in k-space, random motion artifacts, and herringbone artifacts. For the impulse noise artifacts, we generated contaminated k-space measurements retrospectively, and the other two artifacts were reconstructed from real image data.

For a retrospective study of impulse noise artifacts, a real in-vivo data was used. A brain k-space data was obtained with

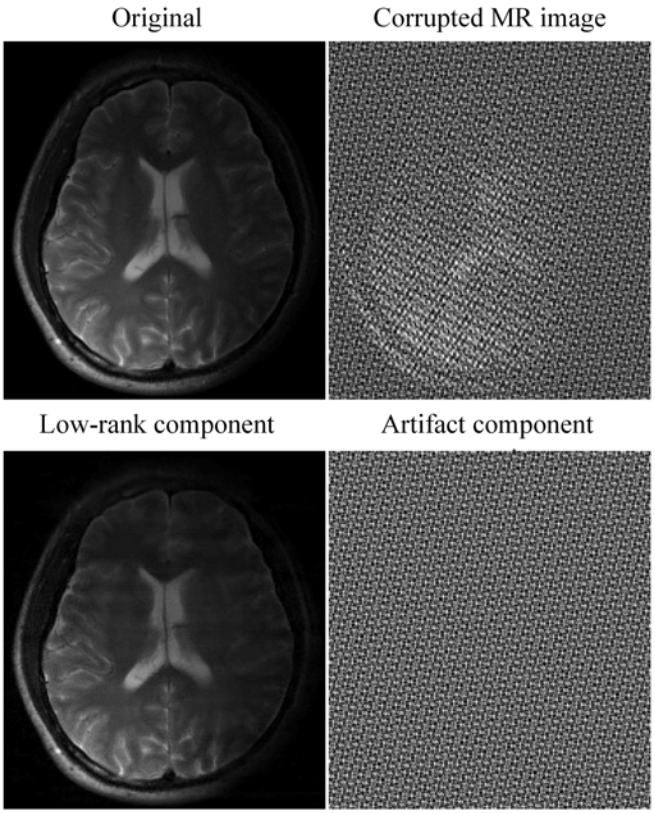

Fig. 2. Reconstruction images and artifacts from five-fold accelerated k-space samples corrupted by impulsive noises.

Siemens Verio 3T scanner using 2D SE sequence. The acquisition parameters were TR/TE = $4000/100$ms, 256×512 acquisition matrix size, 6 z-slice with 5mm slice thickness and FOV was 240×240mm^2, the number of coils was four. Among the four channels, we selected the first coil for our single coil experiment. We added impulse k-space noises for 5 fold accelerated acquisition. A retrospective down-sampling mask was generated by two dimensional Gaussian distribution which includes the central 7×7 region. Fig. 2 clearly showed that the artifacts were clearly removed from the images using the proposed method.

For motion artifact removal experiments, we obtained an image from [7]. Such motion artifact is caused by abrupt motion of object during acquisition. The size of image was 256×256. As observed in Fig. 3, we successfully decomposed image from motion artifacts. As expected, the spectral component from motion artifacts was sparse in spectrum domain.

For Herringbone artifact removal, we obtained an image from [8]. This herringbone artifact appeared as a fabric called herring bone. The size of image is 1024×968. As observed in Fig. 4, we again decomposed true image as a low rank component, whereas the artifacts are decomposed as sparse spectral components. Note that most of artifacts could be successfully

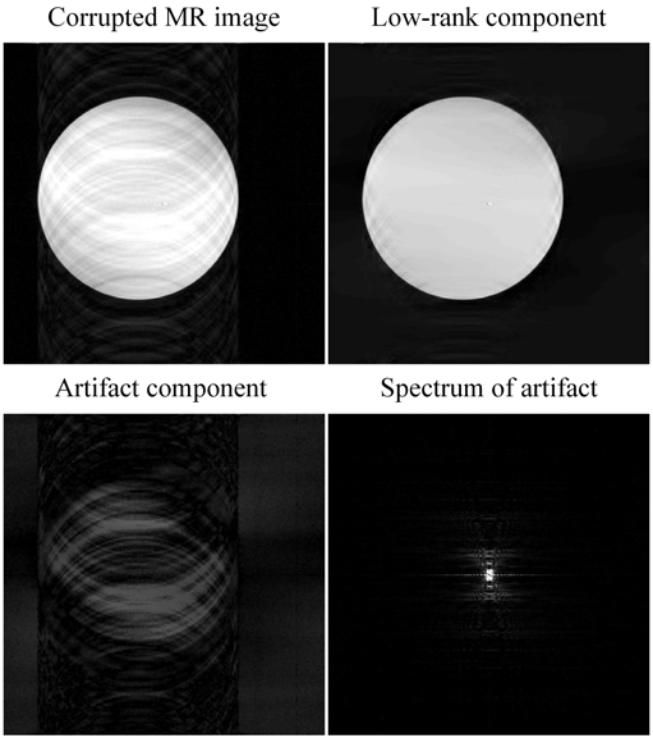

Fig. 3. Reconstruction results of motion artifacts.

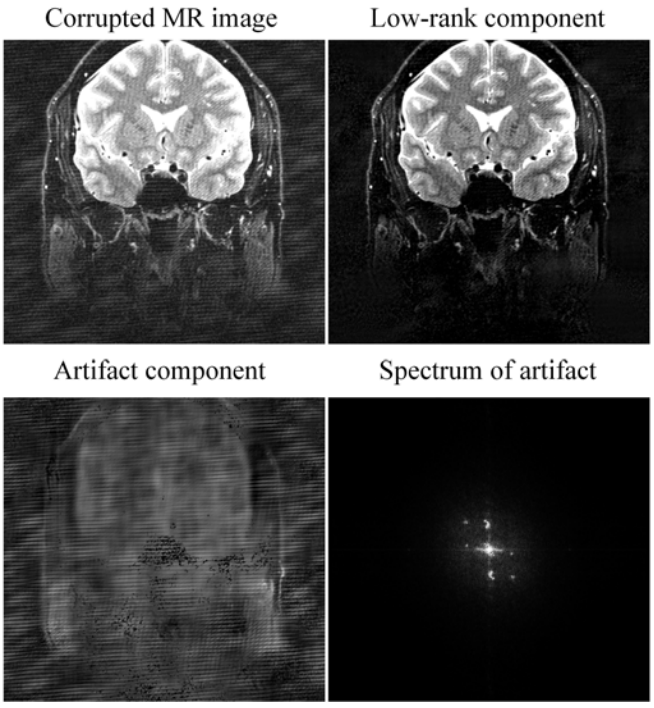

Fig. 4. Reconstruction results of herringbone artifacts.

removed.

In these results, the k-space weighting was very critical. For example, if we decompose corrupted k-space data without k-space weighting, the algorithm failed because the underlying artifact-free image is not sparse in the image domain and the corresponding k-space data cannot be represented as a low-rank Hankel matrix. This again confirms the validity of our theory behind the ALOHA.

4. CONCLUSION

We proposed a novel sparse and low-rank decomposition method for correcting k-space MR artifacts such as motion or random glitch during acquisition. The proposed algorithm successfully decomposed sparse outliers from Hankel matrix. The main principle behind the proposed algorithm is that the underlying artifact-free image can be sparsified in a transform domain, so we can construct a low-rank Hankel matrix using k-space data. Moreover, the sparse outliers in k-space are still sparse, so these components can be removed using a low-rank and sparse decomposition. Using experiments with data corrupted by impulse noises, motion artifact as well as herringbone artifacts, we demonstrated that the algorithm successfully removed the artifacts.

5. REFERENCES

[1] Kyong Hwan Jin, Dongwook Lee, and Jong Chul Ye, "A general framework for compressed sensing and parallel MRI using annihilating filter based low-rank Hankel matrix," *arXiv preprint arXiv:1504.00532*, 2015.

[2] Kyong Hwan Jin and Jong Chul Ye, "Annihilating filter-based low-rank Hankel matrix approach for image inpainting," *IEEE Trans. Image Process.*, vol. 24, no. 11, pp. 3498–3511, Nov 2015.

[3] Ricardo Otazo, Emmanuel Candès, and Daniel K Sodickson, "Low-rank plus sparse matrix decomposition for accelerated dynamic MRI with separation of background and dynamic components," *Mag. Reson. Med.*, vol. 73, no. 3, pp. 1125–1136, 2015.

[4] Greg Ongie and Mathews Jacob, "Off-the-grid recovery of piecewise constant images from few fourier samples," *arXiv preprint arXiv:1510.00384*, 2015.

[5] Emmanuel J Candès, Xiaodong Li, Yi Ma, and John Wright, "Robust principal component analysis?," *Journal of the ACM (JACM)*, vol. 58, no. 3, pp. 11, 2011.

[6] Kyong Hwan Jin and Jong Chul Ye, "Sparse + low rank decomposition of annihilating filter-based Hankel matrix for impulse noise removal," *arXiv preprint arXiv:1510.05559*, 2015.

[7] "chickscope.beckman.uiuc.edu/roosts/carl/artifacts.html," .

[8] "Case courtesy of Dr Roberto Schubert, Radiopaedia.org, rID: 16743," .